

WAVE COMPUTATION ON THE HYPERBOLIC DOUBLE DOUGHNUT*

Agnès Bachelot-Motet

Université de Bordeaux, Institut de Mathématiques, UMR CNRS 5251, F-33405 Talence Cedex
Email: agnes.bachelot@math.u-bordeaux1.fr

Abstract

We compute the waves propagating on the compact surface of constant negative curvature and genus 2 that is a toy model in quantum chaos theory and cosmic topology. We adopt a variational approach using finite elements. We have to implement the action of the fuchsian group by suitable boundary conditions of periodic type. Despite the ergodicity of the dynamics that is quantum weak mixing, the computation is very accurate. A spectral analysis of the transient waves allows to compute the spectrum and the eigenfunctions of the Laplace-Beltrami operator. We test the exponential decay due to a localized dumping satisfying the assumption of geometric control.

Mathematics subject classification: 65M, 65N, 58J, 37D.

Key words: Wave equation, Hyperbolic manifold, Finite elements, Quantum chaos.

1. Introduction

The Hyperbolic Double Doughnut \mathbf{K} is the compact surface of negative constant curvature with two holes. We can define it by the quotient of the hyperbolic Poincaré disc \mathbf{D} , by some Fuchsian group Γ . Alternatively, we can construct it as the quotient of the so-called Dirichlet polygon, or fundamental domain $\mathcal{F} \subset \mathbf{D}$, by a suitable relation of equivalence \sim :

$$\mathbf{K} = \mathbf{D}/\Gamma = \mathcal{F}/\sim .$$

This beautiful object has many fascinating properties as regards the classical and quantum chaos (classical references are [2, 6]). Several important computational investigations of the spectrum were performed by using a stationary method by Aurich and Steiner [1]. Moreover there has been much recent interest for the cosmological models with non trivial topology (a seminal work is the famous “Cosmic Topology” by Lachièze-Rey and Luminet [8]). In this domain, the fluctuations of the cosmic microwave background (CMB) are investigated and we have to compute the evolution of initial metric perturbations. These cosmological questions consist in solving the wave equation on compact multi-connected hyperbolic manifolds, and computing also the eigenvalues and eigenfunctions of the Laplace-Beltrami operator. In this context, \mathbf{K} has been studied as a toy model in [5], where a scheme based on the finite differences on a euclidean grid was used to solve the D’Alembertian. Nevertheless, such a grid appears to be not convenient for the hyperbolic geometry and unsuitable for a description of \mathcal{F} , in particular its boundary. In this paper we compute the solutions of the wave equation in the time domain, by using a variational method and a discretization with finite elements on very fine meshes. The domain of calculus is the Dirichlet polygon, therefore the initial Cauchy problem on the

* Received May 15, 2209 / Revised version received November 3, 2009 / Accepted December 7, 2009 /
Published online August 9, 2010 /

manifold without boundary \mathbf{K} , becomes a mixed problem on \mathcal{F} and the action of the Fuchsian group is expressed as boundary conditions on $\partial\mathcal{F}$, analogous to periodic conditions. These boundary constraints are implemented in the choice of the basis of finite elements. By this way we obtain very accurate results on the transient waves despite the fact that the dynamics is extremely chaotic (the flow is ergodic and quantum weak mixing [13]). We test these results by performing a Fourier analysis of the transient waves that allows to find a lot of eigenvalues of the Laplace-Beltrami operator $\Delta_{\mathbf{K}}$ on \mathbf{K} . We compute also the solutions of the damped wave equation

$$\partial_t^2 \psi - \Delta_{\mathbf{K}} \psi + a \partial_t \psi = 0.$$

When $0 \leq a \in L^\infty(\mathbf{K})$ and $a > 0$ on $\partial\mathcal{F}$, the geometric control condition of Rauch and Taylor [11] is satisfied, and our numerical experiments agree with their theoretical results, stating that the energy decays exponentially.

2. The Hyperbolic Double Doughnut

In this part we describe the construction of the Hyperbolic Double Doughnut. First we recall some important properties of the 2-dimensional hyperbolic geometry. It is convenient to use the representation of the hyperbolic space by using the Poincaré disc

$$\mathbf{D} := \{(x, y) \in \mathbb{R}^2, x^2 + y^2 < 1\},$$

endowed with the metric expressed with the polar coordinates by

$$ds_{\mathbf{D}}^2 = \frac{4}{(1-r^2)^2} dr^2 + 4 \frac{r^2}{(1-r^2)^2} d\varphi^2 = \frac{4}{(1-x^2-y^2)^2} [dx^2 + dy^2].$$

It is useful to use the complex parametrization $z = x + iy$. We have to carefully distinguish the euclidean distance

$$d(z, z') = |z - z'|,$$

and the hyperbolic distance associated to the hyperbolic metric, given by

$$\cosh d_H(z, z') = 1 + \frac{2|z - z'|^2}{(1 - |z|^2)(1 - |z'|^2)}.$$

We remark that

$$d(0, z) = \tanh \frac{d_H(0, z)}{2}$$

hence the euclidean circles centered in 0 are hyperbolic circles centered in 0, and more generally, all the hyperbolic circles $\{z'; d_H(z', z_0) = R\}$, with $R > 0$, $z_0 \in \mathbf{D}$, are euclidean circles. The invariant measure $d\mu_H$ on the Poincaré disc allows to compute the area of any Lebesgue measurable subset $X \subset \mathbf{D}$ by the formula

$$\mu_H(X) = \int_X \frac{4}{(1 - |z|^2)^2} dx dy.$$

The group of the isometries of \mathbf{D} is generated by three kinds of transformations.

1. The Rotations of angle $\varphi_0 \in \mathbb{R}$

$$R_{\varphi_0}(z) = e^{i\varphi_0} z,$$

and so R_{φ_0} is defined in the (x, y) -coordinates by the matrix

$$R_{\varphi_0} = \begin{pmatrix} e^{i\frac{\varphi_0}{2}} & 0 \\ 0 & e^{-i\frac{\varphi_0}{2}} \end{pmatrix}.$$

2. The Boosts, or Möbius transforms, associated with $\tau_0 \in \mathbb{R}$:

$$T_{\tau_0}(z) = \frac{\cosh \frac{\tau_0}{2} z + \sinh \frac{\tau_0}{2}}{\sinh \frac{\tau_0}{2} z + \cosh \frac{\tau_0}{2}}$$

represented in (x, y) -coordinates by the matrix

$$T_{\tau_0} = \begin{pmatrix} \cosh \frac{\tau_0}{2} & \sinh \frac{\tau_0}{2} \\ \sinh \frac{\tau_0}{2} & \cosh \frac{\tau_0}{2} \end{pmatrix}.$$

We remark that

$$\cosh d_H(z, T_{\tau_0}(z)) = 1 + 2 \frac{|z^2 - 1|^2}{(1 - |z|^2)^2} \sinh^2 \left(\frac{\tau_0}{2} \right),$$

therefore

$$\forall z \in (-1, 1), \quad d_H(z, T_{\tau_0}(z)) = |\tau_0|. \tag{2.1}$$

3. The Symmetry

$$S(z) = \bar{z}.$$

Finally we recall that the geodesics of the Poincaré disc are the diameters and all the arcs of circles that intersect orthogonally the boundary of the disc.

Now we are ready to describe the double doughnut that is the quotient of the hyperbolic plane by the Fuchsian group of isometries, Γ , generated by the four transforms g_0, g_1, g_2, g_3 , where

$$g_k = R_{k\frac{\pi}{4}} T_{\tau_1} R_{-k\frac{\pi}{4}}$$

with

$$\tanh \frac{\tau_1}{2} = \sqrt{2(\sqrt{2} - 1)}.$$

The matrix which represents g_k is given by :

$$g_k = \begin{pmatrix} 1 + \sqrt{2} & \sqrt{2 + 2\sqrt{2}} e^{ik\frac{\pi}{4}} \\ \sqrt{2 + 2\sqrt{2}} e^{-ik\frac{\pi}{4}} & 1 + \sqrt{2} \end{pmatrix}.$$

These isometries g_k satisfy the relation :

$$(g_0 g_1^{-1} g_2 g_3^{-1})(g_0^{-1} g_1 g_2^{-1} g_3) = I_d.$$

The *Hyperbolic Double Doughnut* is the quotient manifold

$$\mathbf{K} := \mathbf{D}/\Gamma,$$

endowed with the hyperbolic metric $ds_{\mathbf{K}}^2$ induced by $ds_{\mathbf{D}}^2$. We know, see, e.g., [2, 3, 6], that \mathbf{K} is a two dimensional C^∞ compact manifold, without boundary, its sectional curvature is constant, equal to -1 , and its genus, that is the number of “holes”, is 2. The geodesic flow is very chaotic

: it is ergodic, mixing (theorems by G.Hedlung, E. Hopf), Anosov and Bernouillian (theorems by D. Ornstein, B. Weiss). As regards as these properties of the geodesics flow, we can refer to [2], [3], [6].

To perform the computations of the waves on the doughnut, it is very useful to represent it by a minimal subset $\mathcal{F} \subset \mathbf{D}$ and a relation of equivalence \sim such that

$$\mathbf{K} = \mathcal{F} / \sim .$$

When \mathcal{F} is choosen as small as possible, it is called *Fundamental Polygon*. We take

$$\mathcal{F} := \{z \in \mathbf{D}; \forall i = 0, \dots, 3, |g_i(z)| \geq |z|, |g_i^{-1}(z)| \geq |z|\} .$$

We can see that \mathcal{F} is a closed regular hyperbolic octogon, of which the boundary $\partial\mathcal{F}$ is the union of eight arcs of circle, that are parts of geodesics of \mathbf{D} . As a consequence, the two half-tangents at a vertex are different, hence the vertices are not cusps and the boundary is Lipschitz. We denote $P_j, j \in \mathbb{Z}_8$, the tops of \mathcal{F} , and $\widehat{P_j P_{j+1}}$ the eight edges. The action of Γ on the boundary is described by :

$$\begin{aligned} P_1 &= g_3(P_6), & P_5 &= g_3^{-1}(P_2), \\ P_2 &= g_2(P_7), & P_6 &= g_2^{-1}(P_3), \\ P_3 &= g_1(P_8), & P_7 &= g_1^{-1}(P_4), \\ P_4 &= g_0(P_1), & P_8 &= g_0^{-1}(P_5), \end{aligned} \tag{2.2a}$$

$$\begin{aligned} \widehat{P_1 P_2} &= g_3(\widehat{P_6 P_5}), & \widehat{P_2 P_3} &= g_2(\widehat{P_7 P_6}), \\ \widehat{P_3 P_4} &= g_1(\widehat{P_8 P_7}), & \widehat{P_4 P_5} &= g_0(\widehat{P_1 P_8}). \end{aligned} \tag{2.2b}$$

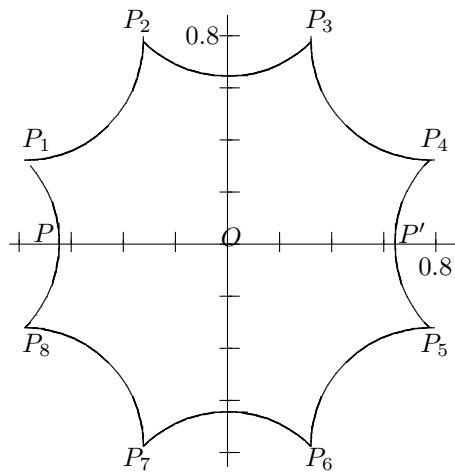


Fig. 2.1: The Fundamental Domain \mathcal{F} .

We define the relation \sim by specifying the class of equivalence \dot{z} of any $z \in \mathcal{F}$, $\dot{z} := \Gamma(\{z\}) \cap \mathcal{F}$, i.e.

$$z \in \mathring{\mathcal{F}} \Leftrightarrow \dot{z} = \{z\},$$

$$\begin{aligned} \dot{P}_j &= \{P_1, P_2, P_3, P_4, P_5, P_6, P_7, P_8\}, \\ z \in \partial\mathcal{F} \setminus \dot{P}_j &\Leftrightarrow \dot{z} = \{z, z_{equiv}\}, \end{aligned}$$

where according (2.2b)

$$z \in \widehat{P_i P_j}, \widehat{P_k P_l} = g_a^{\pm 1}(\widehat{P_i P_j}) \Rightarrow z_{equiv} = g_a^{\pm 1}(z) \in \widehat{P_k P_l}. \tag{2.3}$$

We give some metric relations. Denote $P = \widehat{P_1 P_8} \cap \mathbb{R}^-$ and $P' = g_0(P) = T_{\tau_1}(P)$. We have

$$d_H(P, P') = 2d_H(O, P') = \tau_1,$$

and so

$$\widehat{P_1 P_8} \subset \left\{ z; \left(x + \sqrt{\frac{1 + \sqrt{2}}{2}} \right)^2 + y^2 = \frac{\sqrt{2} - 1}{2} \right\}, \tag{2.4}$$

and by using the rotations we also have :

$$\begin{aligned} d_H(P_i, P_{i+1}) &= \tau_1 = 2d_H(P, P_1) = 2d_H(O, P), \\ d_H(O, P_i) &= \tau_2 \quad \text{with} \quad \tanh \frac{\tau_2}{2} = 2^{-\frac{1}{4}}, \quad d(O, P_i) = 2^{-\frac{1}{4}}. \end{aligned}$$

Finally the area of the fundamental domain is $\mu_H(\mathcal{F}) = 4\pi$.

3. The Waves on the Doughnut

The Laplace Beltrami operator associated with a metric g , is defined by

$$\frac{1}{\sqrt{|g|}} \partial_\mu g^{\mu\nu} \sqrt{|g|} \partial_\nu, \quad g^{-1} = (g^{\mu\nu}), \quad |g| = |\det g_{\mu\nu}|.$$

We consider the lorentzian manifold $\mathbb{R}_t \times \mathbf{K}$ endowed with the metric

$$g_{\mu\nu} dx^\mu dx^\nu = dt^2 - ds_{\mathbf{K}}^2,$$

and we study the covariant wave equation associated to this metric :

$$\partial_t^2 \psi - \Delta_{\mathbf{K}} \psi = 0,$$

More generally, we consider the damped wave equation

$$\partial_t^2 \psi - \Delta_{\mathbf{K}} \psi + a \partial_t \psi = 0, \tag{3.1}$$

with $0 \leq a \in L^\infty(\mathbf{K})$. Here $\Delta_{\mathbf{K}}$ is the Laplace Beltrami operator on \mathbf{K} . Since \mathbf{K} is a smooth compact manifold without boundary, $\Delta_{\mathbf{K}}$ endowed with its natural domain $\{u \in L^2(\mathbf{K}); \Delta_{\mathbf{K}} u \in L^2(\mathbf{K})\}$ is self-adjoint and the global Cauchy problem is well posed in the framework of the finite energy spaces. Given $m \in \mathbb{N}$, we introduce the Sobolev space

$$H^m(\mathbf{K}) := \left\{ u \in L^2(\mathbf{K}), \nabla_{\mathbf{K}}^\alpha u \in L^2(\mathbf{K}), |\alpha| \leq m \right\},$$

where $\nabla_{\mathbf{K}}$ are the covariant derivatives. We can also interpret this space as the set of the distributions $u \in H_{loc}^m(\mathbf{D})$ such that $u \circ g = u$ for any $g \in \Gamma$. Then the standard spectral theory assures that for all $\psi_0 \in H^1(\mathbf{K})$, $\psi_1 \in L^2(\mathbf{K})$, there exists a unique $\psi \in C^0(\mathbb{R}_t^+; H^1(\mathbf{K})) \cap C^1(\mathbb{R}_t^+; L^2(\mathbf{K}))$ solution of (3.1) satisfying

$$\psi(t = 0) = \psi_0, \quad \partial_t \psi(t = 0) = \psi_1, \tag{3.2}$$

and we have

$$\int_{\mathbf{K}} |\partial_t \psi(t)|^2 + |\nabla_{\mathbf{K}} \psi(t)|^2 d\mu_H + \int_0^t \int_{\mathbf{K}} a |\partial_t \psi(t)|^2 d\mu_H dt = Cst.$$

Since $a \in L^\infty(\mathbf{K})$ we have a result of regularity: when $\psi_0 \in H^2(\mathbf{K})$, $\psi_1 \in H^1(\mathbf{K})$, then $\psi \in C^0(\mathbb{R}_t^+; H^2(\mathcal{F})) \cap C^1(\mathbb{R}_t^+; H^1(\mathbf{K})) \cap C^2(\mathbb{R}_t^+; L^2(\mathbf{K}))$.

To perform the numerical computation of this solution, we take the fundamental polygon \mathcal{F} as the domain of calculus. Since the boundary $\partial\mathcal{F}$ is composed of arcs of circles that are intersecting, the vertices are not cusps. Therefore the domain \mathcal{F} is Lipschitz and C^∞ piecewise. We can consider the usual Sobolev space H^m for the euclidean metric,

$$H^m(\mathcal{F}) = \left\{ u \in L^2(\mathcal{F}), \quad \forall \alpha \in \mathbb{N}^2, \quad |\alpha| \leq m, \quad \partial_{x,y}^\alpha u \in L^2(\mathcal{F}) \right\},$$

and given $u \in H^1(\mathcal{F})$, the trace of u on \mathcal{F} is well defined. Therefore the Cauchy problem on $\mathbb{R}_t \times \mathbf{K}$ is equivalent to the mixed problem

$$\partial_{tt}\psi - \frac{(1 - x^2 - y^2)^2}{4} \left[\partial_{xx}\psi + \partial_{yy}\psi \right] + a(x, y)\partial_t\psi = 0, \quad (t, x, y) \in \mathbb{R}^+ \times \mathcal{F}, \tag{3.3}$$

with the boundary conditions

$$\forall (t, z, z') \in \mathbb{R} \times \partial\mathcal{F} \times \partial\mathcal{F}, \quad z \sim z' \Rightarrow \psi(t, z) = \psi(t, z'). \tag{3.4}$$

Given $\psi_0 \in H^1(\mathcal{F})$ satisfying (3.4), and $\psi_1 \in L^2(\mathcal{F})$, there exists a unique $\psi \in C^0(\mathbb{R}_t^+; H^1(\mathcal{F})) \cap C^1(\mathbb{R}_t^+; L^2(\mathcal{F}))$ solution of (3.2), (3.3) and (3.4).

To handle the boundary when applying the finite element method, it is very convenient to take into account the boundary condition (3.4) by a suitable choice of the functional space. We introduce the spaces $W^m(\mathcal{F})$ that correspond to the spaces $H^m(\mathbf{K})$:

$$W^m(\mathcal{F}) := \left\{ u|_{\mathcal{F}}; \quad u \in H_{loc}^m(\mathbf{D}), \quad \forall g \in \Gamma, \quad u \circ g = u \right\},$$

endowed with the norm

$$\|u\|_{W^m} := \|u|_{\mathcal{F}}\|_{H^m(\mathcal{F})}.$$

In particular, we have

$$W^1(\mathcal{F}) = \left\{ u \in H^1(\mathcal{F}), \quad z \sim z' \Rightarrow u(z) = u(z') \right\},$$

and given $m = 1, 2$, for all $\psi_0 \in W^m(\mathcal{F})$, $\psi_1 \in W^{m-1}(\mathcal{F})$, there exists a unique $\psi \in C^0(\mathbb{R}_t^+; W^m(\mathcal{F})) \cap C^1(\mathbb{R}_t^+; W^{m-1}(\mathcal{F}))$ solution of (3.2), (3.3), and we have the energy es-

imate :

$$\int_{\mathcal{F}} \frac{4}{(1-x^2-y^2)^2} |\partial_t \psi(t, x, y)|^2 + |\partial_x \psi(t, x, y)|^2 + |\partial_y \psi(t, x, y)|^2 dx dy + \int_0^t \int_{\mathcal{F}} \frac{4a(x, y)}{(1-x^2-y^2)^2} |\partial_t \psi(s, x, y)|^2 dx dy ds = Cst.$$

When $m = 2$, $\psi \in C^2(\mathbb{R}_t^+; L^2(\mathcal{F}))$, and in this case, the mixed problem can be expressed as a variational problem : ψ is solution iff for all $\phi \in W^1(\mathcal{F})$, we have :

$$\frac{d^2}{dt^2} \int_{\mathcal{F}} \frac{4}{(1-x^2-y^2)^2} \psi(t, z) \phi(z) dx dy + \frac{d}{dt} \int_{\mathcal{F}} \frac{4a(z)}{(1-x^2-y^2)^2} \psi(t, z) \phi(z) dx dy - \int_{\mathcal{F}} \Delta_{x,y} \psi(t, z) \phi(z) dx dy = 0. \tag{3.5}$$

Now the key point consists in expressing in a symmetric manner the last integral, without using an integral on the boundary. To invoke the Green formula, we denote $\nu(z)$ the unit outgoing normal at $z \in \partial\mathcal{F}$. We suppose that $\widehat{P_k P_l} = g_a(\widehat{P_i P_j})$. Then for $z \in \widehat{P_i P_j}$

$$g_a(\nu(z)) = -\nu(g_a(z)).$$

Since $u \circ g_a = u$, we have for $u \in W^2(\mathcal{F})$

$$\partial_{\nu(z)} u(z) = g_a[\nu(z)] \cdot \nabla u(g_a(z)) = -\partial_{\nu(g_a(z))} u(g_a(z)).$$

We deduce that for $u \in W^2(\mathcal{F})$, $v \in W^1(\mathcal{F})$, we have

$$\int_{\widehat{P_i P_j}} v(z) \partial_{\nu(z)} u dz = - \int_{\widehat{P_k P_l}} v(z) \partial_{\nu(z)} u dz,$$

and therefore

$$\int_{\partial\mathcal{F}} v(z) \partial_{\nu(z)} u dz = 0, \int_{\mathcal{F}} \Delta_{x,y} u(z) v(z) dx dy = - \int_{\mathcal{F}} \partial_x u \partial_x v + \partial_y u \partial_y v dx dy.$$

We have proved the following

Theorem 3.1. *Given $\psi_0 \in W^2(\mathcal{F})$, $\psi_1 \in W^1(\mathcal{F})$, the solution ψ of the Cauchy problem (3.1), (3.2), is the unique solution satisfying (3.2) of the variational problem*

$$\forall \phi \in W^1(\mathcal{F}), \frac{d^2}{dt^2} \int_{\mathcal{F}} \frac{4}{(1-|z|^2)^2} \psi(t, z) \phi(z) dx dy + \frac{d}{dt} \int_{\mathcal{F}} \frac{4a(z)}{(1-|z|^2)^2} \psi(t, z) \phi(z) dx dy + \int_{\mathcal{F}} \partial_x \psi(t, z) \partial_x \phi(z) + \partial_y \psi(t, z) \partial_y \phi(z) dx dy = 0.$$

The main advantage of this approach is that the difficulty to fulfilling the boundary condition (3.4), has now disappeared : this condition is replaced by the choice of the space. We solve this

variational problem by the usual way. We take a family V_h , $0 < h \leq h_0$, of finite dimensional vector subspaces of $W^1(\mathcal{F})$. We assume that

$$\overline{\cup_{0 < h \leq h_0} V_h} = W^1(\mathcal{F}).$$

We choose sequences $\psi_{0,h}, \psi_{1,h} \in V_h$ such that

$$\psi_{0,h} \rightarrow \psi_0 \text{ in } W^1(\mathcal{F}), \psi_{1,h} \rightarrow \psi_1 \text{ in } L^2(\mathcal{F}).$$

We consider the solution $\psi_h \in C^\infty(\mathbb{R}_t; V_h)$ of

$$\begin{aligned} \forall \phi_h \in V_h, \quad & \frac{d^2}{dt^2} \int_{\mathcal{F}} \frac{4}{(1-|z|^2)^2} \psi_h(t, z) \phi_h(z) dx dy + \frac{d}{dt} \int_{\mathcal{F}} \frac{4a(z)}{(1-|z|^2)^2} \psi_h(t, z) \phi_h(z) dx dy \\ & + \int_{\mathcal{F}} \partial_x \psi_h(t, z) \partial_x \phi_h(z) + \partial_y \psi_h(t, z) \partial_y \phi_h(z) dx dy = 0, \end{aligned}$$

satisfying $\psi_h(0, \cdot) = \psi_{0,h}(\cdot)$, $\partial_t \psi_h(0, \cdot) = \psi_{1,h}(\cdot)$. Thanks to the conservation of the energy, this scheme is stable :

$$\forall T > 0, \quad \sup_{0 < h \leq h_0} \sup_{0 \leq t \leq T} \|\psi_h(t)\|_{W^1} + \left\| \frac{d}{dt} \psi_h(t) \right\|_{L^2} < \infty.$$

Moreover, when $\psi \in C^2(\mathbb{R}_t^+; W^1(\mathcal{F}))$, it is also converging :

$$\forall T > 0, \quad \sup_{0 \leq t \leq T} \|\psi_h(t) - \psi(t)\|_{W^1} + \left\| \frac{d}{dt} \psi_h(t) - \frac{d}{dt} \psi(t) \right\|_{L^2} \rightarrow 0, \quad h \rightarrow 0.$$

If we take a basis $(e_j^h)_{1 \leq j \leq N_h}$ of V_h , we expand ψ_h on this basis :

$$\psi_h(t) = \sum_{j=1}^{N_h} \psi_j^h(t) e_j^h,$$

and we introduce

$$\begin{aligned} X(t) &:= {}^t(\psi_1^h, \psi_2^h, \dots, \psi_{N_h}^h) \\ \mathbb{M} &= (M_{ij})_{1 \leq i, j \leq N_h}, \quad M_{ij} := \int_{\mathcal{F}} \frac{4}{(1-|z|^2)^2} e_i^h(z) e_j^h(z) dx dy, \\ \mathbb{D} &= (D_{ij})_{1 \leq i, j \leq N_h}, \quad D_{ij} := \int_{\mathcal{F}} \frac{4a(z)}{(1-|z|^2)^2} e_i^h(z) e_j^h(z) dx dy, \\ \mathbb{K} &= (K_{ij})_{1 \leq i, j \leq N_h}, \quad K_{ij} := \int_{\mathcal{F}} \partial_x e_i^h(z) \partial_x e_j^h(z) + \partial_y e_i^h(z) \partial_y e_j^h(z) dx dy. \end{aligned}$$

Then the variational formulation is equivalent to

$$\mathbb{M}X'' + \mathbb{D}X' + \mathbb{K}X = 0.$$

This differential system is solved very simply by iteration by solving

$$\mathbb{M}(X^{n+1} - 2X^n + X^{n-1}) + \frac{\Delta T}{2} \mathbb{D}(X^{n+1} - X^{n-1}) + (\Delta T)^2 \mathbb{K}X^n = 0.$$

We know that this scheme is stable, and so convergent by the Lax theorem, when

$$\sup_{X \neq 0} \frac{\langle \mathbb{K}X, X \rangle}{\langle \mathbb{M}X, X \rangle} < \frac{4}{\Delta T^2},$$

and if there exists $K > 0$ such that

$$\forall h \in]0, h_0], \quad \forall \phi_h \in V_h, \quad \|\nabla_{x,y} \phi_h\|_{L^2(\mathcal{F})} \leq \frac{K}{h} \left\| \frac{2}{1-|z|^2} \phi_h \right\|_{L^2(\mathcal{F})},$$

the CFL condition

$$K\Delta T < 2h$$

is sufficient to assure the stability and the convergence of our scheme.

4. Numerical Resolution

In this part, we present our computational method for solving the Cauchy problem. A crucial step is the construction of the space of finite elements, implementing the action of the Fuchsian group. Another key point is the accuracy of our scheme : although the dynamics is linear, it is extremely chaotic (more precisely $e^{it\sqrt{-\Delta_{\mathbb{K}}}}$ is quantum weak mixing [13]). We test our scheme by computing the spectrum and the eigenfunctions of the Laplacian on the hyperbolic double doughnut by taking the Fourier transform of the transient waves. Finally we test the exponential decay of the damped waves when the microlocal assumption of geometrical control is satisfied.

4.1. Mesh

First of all we construct the boundary $\partial\mathcal{F}$ from the equation (2.4) and we perform a discretization that is equidistant for the hyperbolic metric. Next we use the mesh generators `Emc2TM` and `bamgTM` created by INRIA. If we only use `Emc2TM`, the mesh contains too many vertices and is not suitable for the hyperbolic metric. So a first mesh is created by `Emc2TM`. We also consider a circle which is uniformly discretized with the same hyperbolic step than the exterior geometry. The radius is chosen as the final mesh is almost uniform. At last, we impose on every point of the exterior and interior geometry a metric, in the sense of `bamgTM`. This software can next create a mesh which is more uniform, with respect to the hyperbolic metric, than the first mesh, and that has a reasonable number of vertices.

To test the uniformity of the mesh, we compute the extrema of the hyperbolic distance between two neighbor vertices. As a check of the accuracy of the meshes we evaluated the area of the polygons created by the meshes, and we compared to 4π (area of the domain). Here are some examples:

<i>Mesh</i>	<i>number of vertices</i>	$\max d_H$	$\min d_H$	<i>area/4π</i>
<i>Mesh1</i> :	7448	0.087	0.027	1.00012
<i>Mesh2</i> :	17574	0.049	0.0177	1.00007
<i>Mesh3</i> :	37329	0.036	0.012	1.00003
<i>Mesh4</i> :	67517	0.027	0.009	1.000018

In our meshes, the greater hyperbolic distance between consecutive vertices is not reached near the exterior boundary. To give an idea of the accuracy of this discretization, we show in Figure 4.1, a very rough mesh:

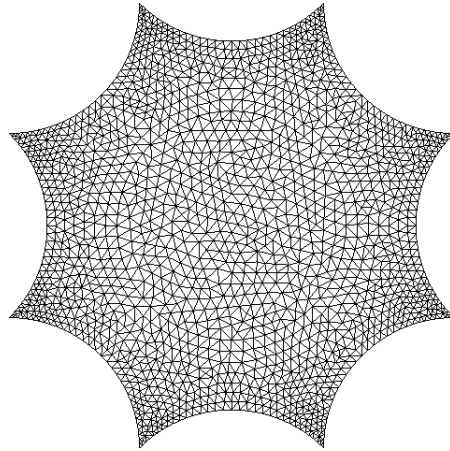


Fig. 4.1: A very rough mesh with 1756 vertices.

4.2. V_h space

We construct the finite element spaces V_h of \mathbb{P}_1 type. The key point consists in implementing the action of the fuchsian group, i.e. we take into account the boundary condition (3.4) in the definition of the finite elements, so that $V_h \subset W^1(\mathcal{F})$. We note \mathcal{T}_h all triangles of a mesh, and $\mathcal{F}_h = \cup_{K \in \mathcal{T}_h} K$, then we introduce :

$$V_h := \left\{ v : \mathcal{F}_h \rightarrow \mathbb{R}, v \in \mathcal{C}^0(\mathcal{F}_h), \forall K \in \mathcal{T}_h v|_K \in \mathbb{P}_1(K), M \sim M' \Rightarrow v(M) = v(M') \right\}.$$

First, we have to determine the equivalent points on $\partial\mathcal{F}$. To that, we write a program implementing the relations (2.3). Finally the number of nodes N_h is the sum $N_1 + N_2 + N_3$, where N_1 is the number of vertices which are not in $\partial\mathcal{F}$, N_2 is the number of vertices which are on four consecutive arcs of $\partial\mathcal{F}$ without being a P_i point, and $N_3 = 1$ because all P_i points are equivalent to one of them.

If j is the number of a node and if M_i denote a vertex of the mesh, we construct a basis $(e_j^h)_{1 \leq j \leq N_h}$ of V_h by:

1. If j is associated to a node that does not belong to $\partial\mathcal{F}$: $e_j^h(M_i) = \delta_{ij}$
So there are N_1 functions of this kind.

2. If j is associated to a node that belongs to $\partial\mathcal{F}$, and is not a P_j point:

$$e_j^h(M_i) = \begin{cases} 1 & \text{if } M_i \sim M_j \\ 0 & \text{otherwise} \end{cases}$$

So there are N_2 functions of this kind.

3. And a last function of the basis associated to the last node: $e_j^h(M_i) = \begin{cases} 1 & \text{if } M_i = P_i \\ 0 & \text{otherwise.} \end{cases}$

4.3. Matrix form of the problem

$\mathbb{K}(i, j)$ and $\mathbb{M}(i, j)$ are found with a numerical integration using the value at the middle of the edges of the triangles. The stiffness matrix \mathbb{K} and the mass matrix \mathbb{M} are sparse and

Table 4.1: $E(n\Delta t)$ with several meshes.

	$E_d(0) :$	$E_d(100) :$	
		with $\Delta t=0.001$	with $\Delta t=0.0005$
<i>Mesh1:</i>	8455.89602005935	8455.89602005865	
<i>Mesh2:</i>	8484.17400988788	8484.17400988815	8484.17400988936
<i>Mesh3:</i>	8494.43409419468	8494.43409419464	8494.43409419511
<i>Mesh4:</i>	8498.39023175937	8498.39023175945	8498.39023175923

symetric matrices. So we choose a Morse storage of their lower part, and all of the calculations will be performed with this storage. To solve the linear problem we use a preconditionned conjugate gradient method. The preconditionner is an incomplete Choleski factorisation, and the starting point is the solution obtained with a diagonal preconditioner.

4.4. Initial data

We consider the case where the initial velocity $\psi_1 = 0$, i.e. $X^0 = X^1 = 0$. We choose different initial data. Some of them have a more or less small support near given points, others are chosen randomly. For the wave depicted in figure 4.2, we have taken

$$\psi_0(x, y) = 100e^{\frac{1}{100x^2+100y^2-1}}, \text{ for } x^2 + y^2 < \frac{1}{100};$$

$$\psi_0(x, y) = \begin{cases} 100 \exp\left(\frac{1}{100x^2 + 100y^2 - 1}\right), & x^2 + y^2 < \frac{1}{100}; \\ 0, & \text{otherwise.} \end{cases} \tag{4.1}$$

And for the one depicted in figure 4.3, we have taken a similar function with a smaller support, and especially a support not centered at the origin. We can see that the last initial data leads to a chaotic behavior.

4.5. Discretized energy

In order to see the stability of our method, we compute $E_d(t)$, the discretized energy at the time t :

$$E(n\Delta t) = \left\langle \mathbb{M} \frac{X^n - X^{n-1}}{\Delta t}, \frac{X^n - X^{n-1}}{\Delta t} \right\rangle + \left\langle \mathbb{K} X^{n-1}, X^n \right\rangle$$

It is well known that our scheme is conservative when $a = 0$, hence E_d must be invariant all along the resolution. We test this property with the previous initial data.

We have performed several movies of transient waves. We constat the temporal chaos predicted by S. Zelditch [13]. In Figure 4.2, the symetries of the initial data are conserved along the time and in Figure 4.3 we can see in the first time that the wave fronts are hyperbolic circles (that are euclidean circles), then after multiple reflections the spatio-temporal chaos appears for a time larger than the diameter of \mathbf{K} that is equal to $2 * d_H(0, P_i) \simeq 4.8969$.

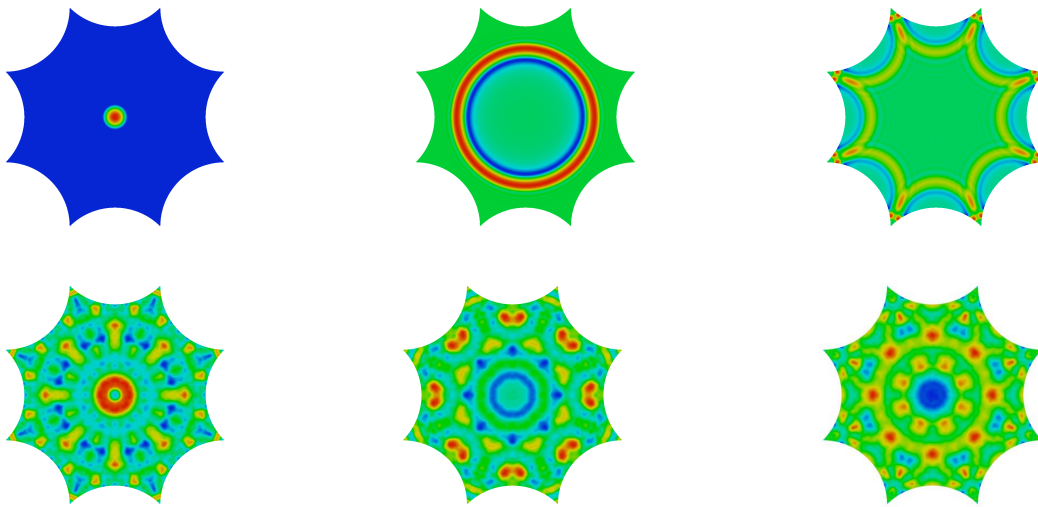


Fig. 4.2: A transient wave at $t = 0, t = 1, t = 2, t = 4, t = 34, t = 99.8$.

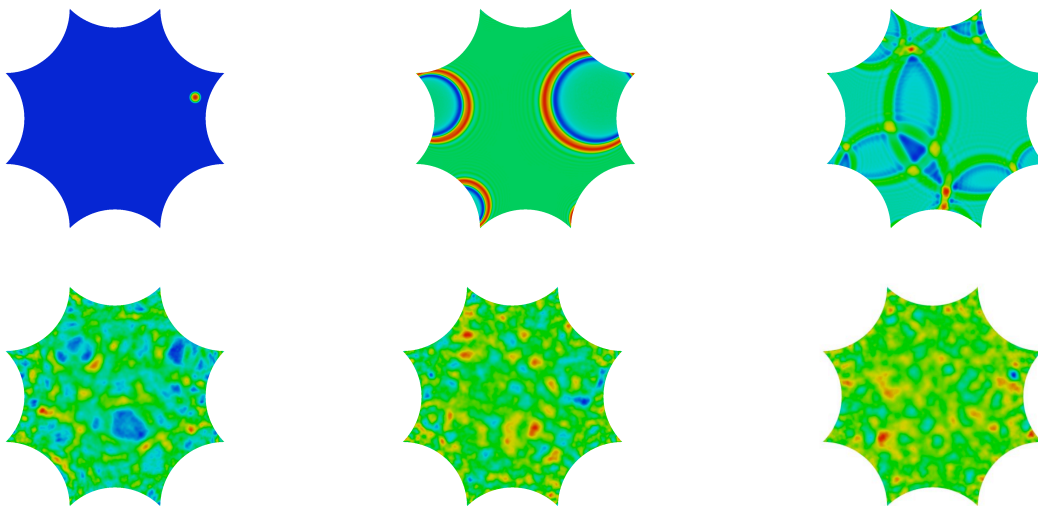


Fig. 4.3: Another transient wave at $t = 0, t = 1, t = 2, t = 4, t = 34, t = 99.8$.

4.6. Eigenvalues

We test our scheme in the time domain, by looking for the eigenvalues of the hamiltonian when $a = 0$. Since the Laplace-Beltrami operator $\Delta_{\mathbf{K}}$ on the Hyperbolic Double Doughnut is a non positive, self-adjoint elliptic operator on a compact manifold, its spectrum is a discrete set of eigenvalues $-q^2 \leq 0$, and by the Hilbert-Schmidt theorem, there exists an orthonormal basis in $L^2(\mathbf{K})$, formed of eigenfunctions $(\psi_q)_q \subset H^\infty(\mathbf{K})$ associated to q^2 , i.e.

$$-\frac{(1-x^2-y^2)^2}{4} \left[\partial_{xx}\psi_q + \partial_{yy}\psi_q \right] = q^2\psi_q, \quad \psi_q \in W^\infty(\mathcal{F}).$$

We take $\psi_0 = \frac{1}{2\sqrt{\pi}}$. Therefore any finite energy solution $\psi(t, X)$ of $\partial_t^2\psi - \Delta_{\mathbf{K}}\psi = 0$ has an expansion of the form $\sum_q e^{iqt}\psi_q(X)$ (such expansions exist also for the damped wave equation, when $a > 0$, see [7]). More precisely, if we denote \langle, \rangle the scalar product in $L^2(\mathbf{K})$, we write

$$\begin{aligned} \psi(t, X) &= \frac{1}{4\pi} (\langle \partial_t\psi(0, \cdot), 1 \rangle t + \langle \psi(0, \cdot), 1 \rangle) \\ &\quad + \sum_{q \neq 0} \langle \partial_t\psi(0, \cdot), \psi_q \rangle \frac{\sin qt}{q} \psi_q(x, y) + \langle \psi(0, \cdot), \psi_q \rangle \cos qt \psi_q(X). \end{aligned}$$

To compute the eigenvalues q^2 , we investigate the Fourier transform in time of the signal $\psi(t, X)$ in the case where $\partial_t\psi(0, X) = 0$. We fix some large $T \gg 1$, and we put

$$\Psi_\omega(X) := \int_0^T \psi(t, X) e^{i\omega t} dt.$$

Then we calculate the square of the modulus of $\Psi_\omega(X)$:

$$\begin{aligned} \|\Psi_\omega\|_{L^2(\mathbf{K})}^2 &= \frac{1}{4\pi} |\langle \psi(0, \cdot), 1 \rangle|^2 + \frac{1}{2} \sum_q \langle \psi(0, \cdot), \psi_q \rangle^2 \left[\frac{\sin^2 \frac{(q+\omega)T}{2}}{(q+\omega)^2} \right. \\ &\quad \left. + \frac{\sin^2 \frac{(\omega-q)T}{2}}{(\omega-q)^2} + \frac{1}{\omega^2 - q^2} (\cos^2 \omega T - \cos \omega T \cos qT) \right]. \end{aligned}$$

Therefore, for an eigenvalue q^2 :

$$\|\Psi_q\|_{L^2(\mathbf{K})}^2 \geq \langle \psi(0, \cdot), \psi_q \rangle^2 \left(\frac{T^2}{4} - \frac{T}{2q} \right),$$

and we look for ω such that $\|\Psi_\omega\|_{L^2(\mathbf{K})}^2 \gg 1$. Practically, during the time resolution of the equation, we store the values of the solution at all vertices $M(X)$ for the discrete time $k\Delta t$, $N_i \leq k \leq N_f$. We choose the initial step N_i in order to the transient wave is stabilized, that to say $N_i\Delta t$ is at least greater than the diameter of the doughnut, i.e.,

$$N_i\Delta t \geq 2 * d_H(0, P_i) \simeq 4.8969.$$

Then we compute a DFT of $(\psi_h(k\Delta t, X))_{N_i \leq k \leq N_f}$ with the free FFT library `fftw`. Let us note $(\Psi_j(X))_{0, N_f - N_i + 1}$ the result. We then obtain $\|\Psi_j(X)\|_{L^2}$. From the foregoing we search the values $jmax_1, jmax_2, \dots$ for which $\|\Psi_j(X)\|_{L^2}$ has a maximum. Then the eigenvalues found by the algorithm are expressed as:

$$q = \frac{2\pi}{(N_f - N_i + 1)\Delta t} jmax.$$

The uncertainty on the value of q is related to $(N_f - N_i + 1)\Delta t$. In most of our results it is equal to 0.07. In order to reduce the uncertainty we have to resolve the equation on a greater time interval. We have made a lot of tests by varying parameters such as: $\Delta t, N_i$, mesh, initial data. Depending on the choice of the initial data, all the modes are not excited. For a given mesh and a given N_i large enough, the numerical value of an eigenvalue does not vary with initial data, up to the twelfth decimal place. By using our temporal method based on the transient waves, we obtain a lot of eigenvalues q^2 that we give in Table 4.2, in which we present also the numerical values obtained with a stationary method with a mesh of 3518 vertices in [1]. We can see a good agreement. Nevertheless two eigenvalues are missing, 75.53 and 86.71. To explain this fact, we remark that the difference between these eigenvalues and their closest neighbors, 75.67 and 86.18 is smaller than the uncertainty on q^2 of our own method that cannot distinguish these both values.

Table 4.2: Eigenvalues q^2 obtained by using our temporal method.

Temporal	Stationary	Temporal	Stationary	Temporal	Stationary
3.821	3.8388	36.047	36.238	71.36	71.42
5.307	5.353	38.606	38.96	73.73	73.66
8.193	8.249	40.360	40.11	74.94	74.92
14.743	14.726	43.065	42.85		75.53
15.284	15.048	43.98	44.01	76.15	75.67
18.735	18.658	50.71	50.55	86.21	86.18
20.592	20.519	57.90	57.48		86.71
23.204	23.078	59.6	59.46	91.47	91.46
28.151	28.079	61.14	61.02	94.16	93.37
31.193	30.833	62.23	62.63	98.27	97.87
32.772	32.673	67.86	67.61	101.06	100.70

4.7. Eigenfunctions

We next perform some eigenfunctions ψ_q associated to the first non zero eigenvalue q . $\psi_q(X)$ is obtained as:

$$\psi_q(X) = \lim_{T_f - T_i \rightarrow +\infty} \frac{1}{T_f - T_i} \int_{T_i}^{T_f} \psi(t, X) e^{-iqt} dt$$

We take T_i twice larger than the diameter of the hyperbolic doughnut and $T_f \sim 100$.

We find the three following linearly independent eigenfunctions; they are obtained with transient solutions $\psi(t, \cdot)$ corresponding to different initial data $\psi(0, X)$, see Figure 4.4.

Moreover any of the other eigenfunctions that we find are numerically dependent with these three ones. We conclude that the ground state is degenerated, with multiplicity 3. That is

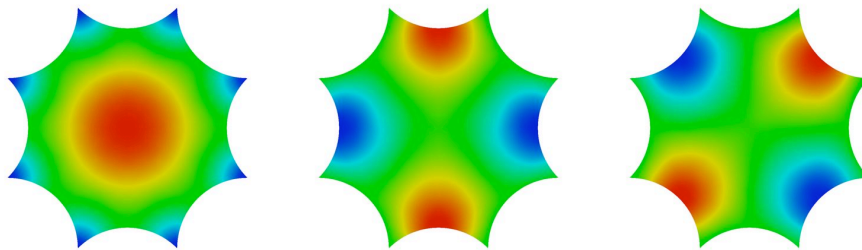


Fig. 4.4: Three independent eigenfunctions associated to the first non zero eigenvalue.

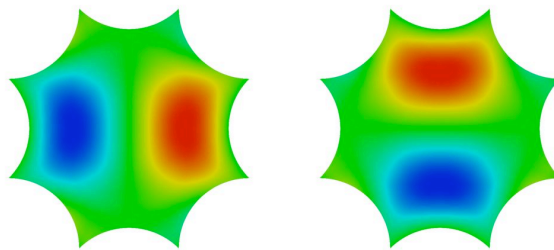


Fig. 4.5: Two independent eigenfunctions associated to the second non zero eigenvalue.

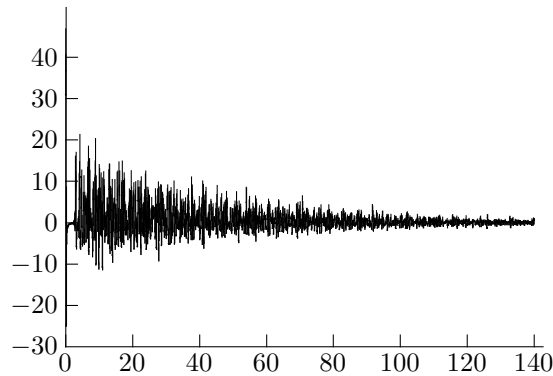


Fig. 4.6: Solution at the origin.

in agreement with the stationary computations by [1]. With a judicious choice of initial data we also find two independent eigenfunctions associated to the second non zero eigenvalue, see Figure 4.5.

4.8. Damped waves

We test our scheme for the damped wave equation (3.1) when the damping function $a \geq 0$ is non zero (for deep theoretical results, see, e.g., [7, 9, 11, 12]). We know that the energy of any finite energy solution decays exponentially (uniformly with respect to the initial energy) if the dumping a satisfies the assumption of geometric control introduced by Rauch and Taylor in [11]. This condition means

$$\int_0^\infty a(x(t), y(t)) dt = +\infty \quad (4.2)$$

for any geodesic $(x(t), y(t))$. Because of the properties of the geodesic flow, it is sufficient to have $a > 0$ on $\partial\mathcal{F}$.

Figures 4.6 and 4.7 are obtained with the initial data 4.1, Mesh3 and a is defined by:

$$a(x, y) = 0, \text{ for } |z| < 0.6 ; \quad a(x, y) = 0.1, \text{ otherwise.}$$

We can see that the solution is strongly oscillating, fast decreasing and we note an excellent agreement with the theorem of exponential decay of the energy. Since Hitrik has proved in [7] that under the assumption of geometric control, the propagator admits an expansion in terms

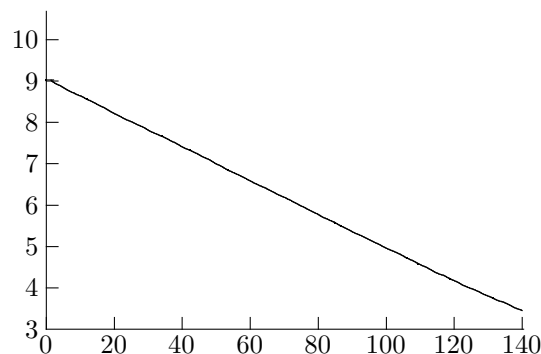


Fig. 4.7: Logarithm of the energy as a function of time.

of finitely many eigenmodes near the real axis, with an error term exponentially decaying in time, the solution can be expressed as

$$\Psi(t, x, y) \underset{q}{\overset{\sim t \rightarrow \infty}{\sum}} e^{iqt} c_q(x, y), \quad \text{Im}(q) > 0; \quad \text{as } t \rightarrow \infty.$$

Then we could use our resolution in the time domain, to determine the spectrum of the hamiltonian, by applying the method of computation of the resonances, based on the Prony algorithm, that we have developed in [10] for the Schwarzschild black-holes quasi-normal modes.

4.9. Conclusion

We have validated a computational method for the transient waves on the hyperbolic double doughnut. Despite the ergodic properties of the dynamics, the computations are very precise and allow also to obtain the eigenmodes. We plan to implement hyperbolic curve triangles, and higher order finite elements to improve the accuracy again, in the spirit of the methods by G. Cohen [4].

The hyperbolic double doughnut can be considered as a toy-model of the more realistic cases arising in the cosmology of the multi-connected universes. The main challenge in this domain consists in detecting the gravitational waves, since the spectrum of the eigenfrequencies of these waves, characterizes the unknown topology of the universe. When these waves are measured, the comparison with the waves computed for special models, provides information on the nature of our world. Hence the computation of the solutions of the d'Alembertian on some lorentzian manifolds, with a non trivial topology, is a crucial step. In particular it will be interesting to compute the waves propagating on a three dimensional hyperbolic compact manifold. There is no difference of principle with the case that we have treated in this paper. We can adopt the same method by replacing $\mathbf{K} = \mathbf{D}/\Gamma = \mathcal{F}/\sim$ by \mathbf{B}/Γ' where \mathbf{B} is the Poincar 3D-ball, and Γ' some Fuchsian group. The only change is the increased complexity, since the fundamental domain \mathcal{F} becomes 3-dimensional, and we have to replace the triangles of the 2-D mesh, by tetrahedra. Then we shall be able to compare our computations with the observations of the fluctuations of the cosmic microwave background.

References

- [1] R. Aurich and F. Steiner, Periodic-orbit sum rules for the Hadamard-Gutzwiller model, *Phys. D*, **39** (1989), 169-193.
- [2] N.L. Balazs and A. Voros, Chaos on the pseudosphere, *Phys. Rep.*, **143**:3 (1986), 109-240.
- [3] M.B. Bekka and M. Mayer, *Ergodic Theory and Topological Dynamics of Group Actions on Homogeneous Spaces*, London Mathematical Society Lecture Notes Series, Cambridge University Press, **269** (2000).
- [4] G.C. Cohen, Higher-Order Numerical Methods for Transient Wave Equations, Scientific Computation, Springer-Verlag, 2002.
- [5] N.J. Cornish and N.G. Turok, Ringing the eigenmodes from compact manifolds, *Classical. Quant. Grav.*, **15** (1998), 2699-2710.
- [6] M.C. Gutzwiller, *Chaos in Classical and Quantum Mechanics*, Interdisciplinary Applied Mathematics, Springer-Verlag, **1** (1990).
- [7] M. Hitrik, Eigenfrequencies and expansions for damped wave equations, *Methods Appl. Anal.*, **10**:4 (2003), 543-564.

- [8] M. Lachièze-Rey and J.P. Luminet, Cosmic Topology, *Phys. Rep.*, **254** (1995), 135-214.
- [9] G. Lebeau, Equations des ondes amorties, *Séminaire X-EDP*, Ecole Polytechnique, **15** (1994).
- [10] A. Motet-Bachelot, Resonances of the Schwarzschild metric, in *Nonlinear evolutionary partial differential equations (Beijing, 1993)*, Xia-Xi Ding, Tai-Ping Liu (ed.), *AMS/IP Stud. Adv. Math.*, Amer. Math. Soc., Providence, RI, **3** (1997), 483-487.
- [11] J. Rauch and M. Taylor, Decay of solutions to nondissipative hyperbolic systems on compact manifolds, *Commun. Pur. Appl. Math.*, **28** (1975), 501-523.
- [12] E. Schenck, Energy decay for the damped wave equation under a pressure condition, (2009), arXiv:0909.2093v1.
- [13] S. Zelditch, Quantum mixing, *J. Funct. Anal.*, **140** (1996), 68-86.